Supplementary Material to Andrés-Blasco, Vinué et al. "**Hepatic lipase inactivation decreases atherosclerosis in insulin resistance by reducing LIGHT/Lymphotoxin β-Receptor pathway" (Thromb Haemost 2016; 116.2)**

Suppl. Methods

Metabolic measurements in mice

Plasma lipid levels in overnight-fasted mice were measured using enzymatic procedures (Wako). HDL-cholesterol (HDL-C) was determined after precipitation of the apolipoprotein B-lipoproteins with dextran sulphate as described(1, 2). Glucose tolerance test (GTT), was performed by intraperitoneal injection of glucose (2 g/Kg of body weight, BW) in overnight-fasted mice and plasma glucose and insulin levels were analysed at different time-points using a glucometer (Ascensia Elite, Bayer) and an ultrasensitive anti-mouse insulin ELISA (Mercodia). Insulin tolerance test (ITT), was performed in 4 h-fasted mice by intraperitoneal injection of insulin (0.75U/Kg of BW ACTRAPID) and glucose levels were measured.

In vivo foam cell determination in peritoneal lavage

For in vivo foam cell determination, mice were anesthetised with inhalational anesthesia (5% and 2% of isofluorane during the procedure) and freshly isolated resident peritoneal macrophages were plated on coverslips for 60 minutes and extensively washed to remove nonadherent cells. After fixation with PFA4%/PBS, cells were stained with Oil Red-O, counterstained with hematoxylin and mounted with glycerol-gelatin.

Immunohistopathological analysis of atheromas in cross-sections

Masson's trichrome staining in cross-sections was used to determine collagen, necrotic core area and fibrous cap thickness. Necrotic cores were defined as non-stained and acellular areas in the Masson's stainings and fibrous cap thickness was the average of 3-5 thickness values of regions above the necrotic cores as previously described (3). Macrophages were detected with a rat anti-Mac-3 monoclonal antibody (1/200, sc-19991, SantaCruz Biotechnology), followed by biotin-conjugated goat anti-rat secondary antibody (1/300, sc-2041, SantaCruz Biotechnology), streptavidin-HRP (TS-060-HR, LabVision) and DAB substrate (SK4100, Vector Laboratories). Slides counterstained with hematoxylin were mounted with EUKITT (A10500, Deltalab). Images were captured with an OPTIKAMPRO5 digital camera mounted on a stereo microscope (Optika) and analysed by computer-assisted morphometry with Image J (4).

Proliferating macrophages in lesions from aortic cross-sections were detected by double immunofluorescence for Ki67/F4/80 which consisted of antigen retrieval with Sodium Citrate buffer (10mM, pH 6.5 at high pressure and temperature), blocking (horse serum 5%, 1h at room temperature, RT), incubation with primary antibodies (overnight at 4ºC, rabbit monoclonal anti-Ki67 antibody Clone SP6, MAD-000310QD, VITRO; rat anti-F4-80: 1/50, MCA497G AbDSerotec) followed by incubation (1h at RT) with goat anti-rat IgM AlexaFluor-594 and anti-rabbit IgG AlexaFluor-488 (1/200, A21213 and A21206, LifeTechnologies) secondary antibodies. For Lymphotoxin beta receptor (LTβ-R) expression a rabbit polyclonal antibody anti-LTβ-R (1/200, ab70063, Abcam) combined with a rat anti-F4/80 followed by secondary antibodies goat anti-rat IgM AlexaFluor-594 and anti-rabbit IgG AlexaFluor-488. T-lymphocytes were detected by inmunofluorescence using the polyclonal anti-human CD3 antibody (1/75, A0452, Dako) and secondary antibody AlexaFluor-488 anti-rabbit IgG (1/200, A21206, LifeTechnologies). Nuclear staining was performed with 4',6-diamidino-2-phenylindole (DAPI) (D1306, LifeTechnologies) and slides were mounted with Slow-Fade Gold reagent (S36936, Invitrogen) and analysed with an inverted fluorescent microscope.

Enzyme-Linked ImmunoSorbent Assay (ELISA)

Plasma was isolated by centrifugation of heparinised blood. Circulating plasma levels of TNF-α, MCP1 and IL6 were measured using the Quantikine ELISA kits (R&D Systems) and circulating LIGHT was quantified using a mouse-specific anti-LIGHT ELISA kit (antibodies-online GmbH). In human plasma LIGHT was determined using the anti-LIGHT DuoSET ELISA development system (R&D Systems).

Bone marrow-derived macrophage cell culture, proliferation assay and wound-healing migration assays

Murine bone marrow-derived macrophages were obtained from femoral bone marrow of mice sacrificed by cervical dislocation. Cells were differentiated during 7 days with 10%FBS/DMEM 10% L929-cell conditioned medium (LCM, source of macrophage colony-stimulating factor) as described (4). Proliferation was evaluated in *apoE-/-Irs2+/-HL-/-* and *apoE-/-Irs2+/-HL+/+* macrophages by 18h-incorporation of bromodeoxyuridine (BrdU, 50 µM, Sigma) into macrophages grown on coverslips detected with a monoclonal anti-BrdU AlexaFluor-488 antibody (clone MoBU-1, B35130, Invitrogen) on fixed (PFA 4%/PBS) and permeabilised (0.5% Triton X-100, 2 M HCL) cells (4). The proliferation rate was determined as a percentage of BrdU-positive cells relative to the total cell count determined in DAPI-stained cells. Data shown is the average of all 9-12 coverslips (300-500 cells/coverslip). Migratory activity was determined by the wound-healing assay (3) in plates grown to 80% confluence. Before assay, cells were treated with Mitomycin C (10 µg/mL, SIGMA, St. Louis, MO, USA) for 1 h. At time 0, a wound was made in the middle of the cell monolayer using a sterile tip and cells were incubated in 0.5% FBS/DMEM 10% LCM for 24h and pictures were taken at time 0h and 24h. Differences between groups were assessed as wound area at time t24 relative to wound area at t0 (area t0 equal to 100%) in 4 independent fields in eight independent wells per genotype.

Treatment of *apoE-/-* mouse macrophages with murine LIGHT

ApoE-/- mouse macrophages were obtained as above, differentiated during 5 days and incubated with 100 ng/mL of murine LIGHT in 0.5% FBS 10% L929/DMEM P/S/A media for 24h and analysed by Western Blot and qPCR.

Gene expression analysis by quantitative real-time PCR (qPCR)

RNA was obtained with TRIzol Reagent (Invitrogen) from bone marrow-derived macrophages, from snap-frozen aortic arch and from human WBMCs, isolated from peripheral blood samples with Ficoll-Hypaque density gradient centrifugation (GE HealthCare, ThermoFisher, Barcelona, Spain). RNA was retrotranscribed with Maxima First Strand cDNA Synthesis kit and amplified with Luminars Color HiGreen(High ROX)-qPCR Master MIX (Fermentas). Reactions were run on a thermal Cycler 7900Fast System and analysed with the software provided (Applied Biosystems). The primers designed with the Primer Express program (Applied Biosystems) were: murine *Light*: Fw 5´-CTCCAGACTTGCCACCACA-3´, Rv 5´-GGTGGCTGGAAACCAATGC-3´; murine *Ltβ-r*: Fw 5´-GCAAGCCTGAGACCTAGTTTCAG-3´, Rv 5´-CCTTGTGTCCGAGGCTCAAT-3´; murine *cyclophilin*: Fw 5'-TGGAGAGCACCAAGACAGACA-3', Rv 5'-TGCCGGAGTCGACAATGAT-3'; murine *Tnf-α*: Fw 5'-CCCACACCGTCAGCCGATTT-3' Rv 5'-GTCTAAGTACTTGGGCAGATTGACC-3'; murine *Mcp1:* Fw 5'-GCCCAGCACCAGCACCAG-3', Rv 5'-GGCATCACAGTCCGAGTC-3'; murine $p15^{Ink4b}$: Fw 5′-AGATCCCAACGCCCTGAAC-3', Rv 5′-CCCATCATCATGACCTGGATT-3′; murine $p16^{Ink4a}$: Fw 5′-CGTACCCCGATTCAGGTGAT-3´, Rv 5′-TTGAGCAGAAGAGCTGCTACGT-3′. Human g*apdh:* Fw 5'-ACCACAGTCCATGCCATCAC-3' and Rv 5'-TCCACCACCCTGTTGCTGTA-3'; human *Ltβ-r*: FW 5'-GAGGGACCCAATCCTGTAGCT -3' and Rv 5'-TGTACCAAGTCAGGGAAGTATGGA-3'. Human *Hl*: FW 5'-CCCTGCCTCTGGTGATGATAA-3' and Rv 5'-TGCCAGATCCAGTTTTCTAGC -3'.

Human subjects

Recruitment of human samples was selected by opportunistic method and subjects were classified as Metabolic syndrome (MetS) patients following the criteria defined by the National Cholesterol Education Program (NCEP)-Adult Treatment Panel (ATP)III (5). MetS patients with homeostatic model assessment (HOMA) index ≥3.2 were considered insulin resistant (IR) (6). Using this criteria, 65 MetS subjects with IR and 56 MetS individuals without IR were identified. Blood samples collected after 12–14 h of fasting were drawn from an antecubital vein in tubes containing EDTA (BD Vacutainer, Plymouth, UK) and were centrifuged within 4h. Biochemical parameters were measured by standard methodology by the Hospital Clinic. Insulin was determined by radioimmunoassay.

Human carotid artery ultrasound evaluation

B-mode ultrasound imaging of the right and left carotid arteries was performed using a Siemenes Sonoline G40 instrument (Siemens Medical Solutions, Erlangen, Germany) equipped with 7 to 10-MHz broadband linear array transducers. Patients were examined in the supine position with the head turned 45° contralateral to the side of scanning. Before obtaining images for intima-media thickness (IMT) measurements, B-mode and color Doppler sonographic examinations were done in longitudinal and transverse planes to identify vascular stenoses. A standardized imaging protocol was used for the IMT measurements in agreement with the Mannheim consensus (7). With the carotid dilatation and flow dividers as anatomic landmarks, the sonographer obtained high-resolution images of the common carotid (1 cm proximal to the bifurcation), the bifurcation (between dilatation and flow divider), and the internal carotid (1 cm distal to the flow divider). Analysis of external and internal carotid artery and carotid bifurcation was analysed for the presence of atherosclerotic plaques and analysis of the echogenicity. Atherosclerotic plaque was defined as a focal structure that encroaches into the arterial lumen of at least 0.5 mm, 50% of the surrounding IMT value or a thickness of > or =1.0 mm as measured from the media-adventitia interface to the intima-lumen interface. The primary variable was mean common carotid IMT (CC-IMT), defined as the average of distances between the far wall lumen-intima and media-adventitia ultrasound interfaces taken bilaterally, in three different projections (right common carotid artery: 90º, 120º and 150º; left common carotid artery: 210º, 240º and 270º). An experienced sonographer (S.M.-H.) performed all examinations. Intraobserver variability was examined in 20 subjects. The coefficient of variability of mean CC-IMT was 5.2%.

Flow cytometry measurements

For determination of circulating leukocytes in mice, 10µl of heparinised whole blood were incubated 30 min at RT with Ly6C-PerCP (BD Pharmingen) and CD115-APC (Biolegend) antibodies or with 5 µl Brilliant Stain Buffer (563794, BD) and with the following antibodies: rat anti-mouse CD4-BV (562891, BD), rat anti-mouse CD8a-BV (563068, BD), anti-mouse CD69-PE (553237, BD) and anti-mouse CD3e-APC (553066, BD). Incubation with lysing solution was done before analysis by flow cytometry (FACSVerse Flow cytometer, BD). Analysis of $Ly6C^{low}$ and $Ly6C^{hi}$-monocyte subsets were determined in CD115+ populations as described (8). Total leukocytes, lymphocytes and neutrophils were identified by morphology and monocytes by the CD115 marker. To characterise circulating human monocytes 10 µl of heparinised whole blood was incubated 30 min at room temperature with V450 mouse anti-human CD14 and PerCP-Cy5.5 mouse anti-human CD16 (BD Pharmingen) followed by 5 minutes incubation at RT with lysing solution (BD Facs Lysing solution) and analysed by flow cytometry (FACSVerse Flow cytometer, BD Biosciences). Monocytes were gated as previously described to differentiate between the three populations classical CD14++CD16-, intermediate CD14++CD16+, which both are inflammatory, and alternative or anti-inflammatory CD14+CD16++ (9).

Culture and silencing of human monocytes-derived macrophages

Human peripheral blood mononuclear cells (PBMCs) were isolated from peripheral blood samples of healthy volunteers with Lymphoprep density gradient centrifugation (Axis Shield PoC, Oslo, Norway), plated in cell plates with 15% FBS RPMI1640-Penicillin/Streptomycin/Amphotericin (P/S/A) and maintained in a humidified 5% CO_2 atmosphere for 1 hour. After 1 hour, non-adherent cells which contained lymphocytes were removed and monocyte-adhered cells were kept for 5-7 days for macrophage differentiation in the presence of the same RPMI media (10).
For gene silencing with small interfering RNA (siRNA), monocyte-derived macrophages grown to 50-60% confluency were transfected with human control or human LIPC-specific siRNA (ON-TARGET PLUS, SMART POOL, Dharmacon, Lafayette, CO, USA) using lipofectamine RNAiMAX (Invitrogen, Carlsbad, CA, USA) for 48h. siRNA macrophages were treated with 100ng/mL of human LIGHT (R&D Systems) in 0.5% FBS RPMI 1640-P/S/A media for 24h and then analysed by mRNA gene expression analysis. Monocyte/macrophage culture purity was confirmed by flow cytometry as described above.

Western Blot analysis

Liver and macrophage protein lysates were obtained in the presence of the ice-cold lysis TNG buffer (Tris-HCl 50 mM, pH7.5, NaCl 200 mM, Tween-20 1%, NP-40 0,2%) supplemented with Complete Mini cocktail, PhosSTOP (Roche, Mannheim, Germany), ß-glicerolphosphate 50 mM (SIGMA), 2 mM phenylmethylsulfonyl Fluoride (PMSF, ROCHE, Mannheim, Germany) and 200 µM Na3VO4 (SIGMA). Protein extracts (100-300 µg) were prepared in laemmli's buffer and analysed by 12% polyacrilamide gel electrophoresis and western blot (3, 11). The primary antibodies used were: rabbit polyclonal anti-Phospho-p38 (1/200, sc-17852-R, SantaCruz Biotechnology), rabbit polyclonal anti-p38 (1/200, sc-535, SantaCruz Biotechnology), rabbit polyclonal hepatic lipase (H-70) (D1/100, sc-21007, SantaCruz Biotechnology) and mouse anti-β-actin (1/500, A5441, Sigma). The HRP-conjugated secondary antibodies (1/500, SantaCruz Biotechnology) used were: anti-mouse IgG-HRP (sc-2005) and goat anti-rabbit IgG-HRP (sc-2004). The immunocomplexes were detected with an ECL Plus detection kit (ThermoFisher Scientific, Barcelona, Spain).

Suppl. Table 1. Demographic and clinical characteristics of human subjects.

	MetS	MetS-IR	p value
N (F/M)	56 (36/20)	65 (35/30)	
Age (years)	59.1 ± 8.7	56.1 ± 8.6	
SBP (mmHg)	138.3 ± 17.2	138.0 ± 16.7	
DBP (mmHg)	81.6 ± 9.1	85.5 ± 10.4	
BMI	28.6 ± 4.2	32.4 ± 5.2*	<0.001
Waist Circunference (cm)	94.7 ± 10.6	104.4 ± 13.1*	<0.001
Fasting Glucose (mg/dL)	98.6 ± 13.7	124.2 ± 32.0*	<0.001
Insulin (mU/L)	8.9 ± 2.7	20.6 ± 9.0*	<0.001
HOMA index	2.1 ± 0.7	6.3 ± 3.3*	<0.001
Total Cholesterol (mg/dL)	225.8 ± 57.7	231.3 ± 43.8	
Triglycerides (mg/dL)	147.9 ± 72.6	234.6 ± 162.8*	<0.001
HDL-C (mg/dL)	56.1 ± 12.3	47.6 ± 9.1*	<0.001
LDL-C (mg/dL)	142.2 ± 49.5	145.6 ± 36.0	
Apo B (mg/dL)	107.4 ± 31.6	112.3 ± 23.2	
hsCRP (mg/dL)	2.3 ± 1.9	3.3 ± 2.4	
Fibrinogen	4.2 ± 0.8	4.2 ± 0.9	
Obesity (%)	30.4	59.4	
Diabetes (%)	10.7	40*	<0.001
Dyslipidemia (%)	82.1	81.5	
Hypertension (%)	61.8	69.5	<0.0001
Medication			
Antihypertensives(%)	48.2	46.2	
Lipid-lowering(%)	42.9	29.2*	<0.007
Oral hypoglycemics (%)	8.9	29.2*	<0.0001

*Significant differences between MetS and MetS-IR patients; BMI: body mass index; SBP: systolic blood pressure; DBP: dyastolic blood pressure; LDL-C: low density lipoprotein cholesterol; HDL-C: high density lipoprotein cholesterol; apoB: apolipoprotein B; hsCRP: high sensitive C-reactive protein.

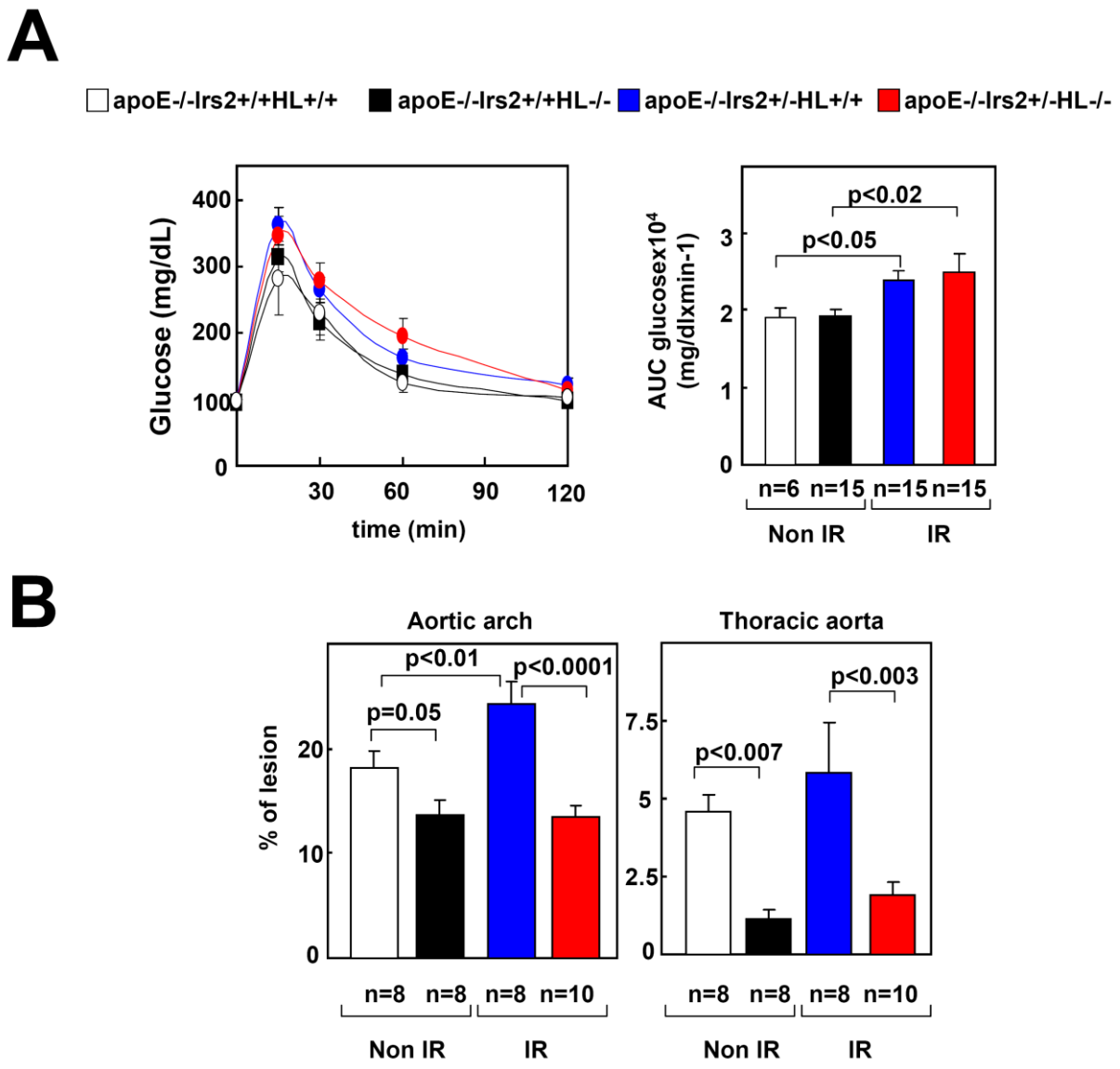

Suppl. Figure 1. Metabolism and atheroma development in MetS/IR *apoE-/-Irs2+/-* and *apoE-/-Irs2+/-HL-/-* mice and non-IR mice *apoE-/-* and *apoE-/-HL-/-* mice mice fed atherogenic diet for two months. (A) Glucose levels during the GTT (left panel) and Area Under the Curve ($AUC_{glucose}$) parameter in all four groups of mice. Analysis of the $AUC_{glucose}$ demonstrates that *Irs2* haploinsufficiency in both *apoE-/-Irs2+/-HL+/+* and *apoE-/-Irs2+/-HL-/-* produces glucose intolerance as compared with mice with intact *Irs2*, *apoE-/-Irs2+/+HL+/+* and *apoE-/-Irs2+/+HL-/-* mice ($p<0.05$ and $p<0.02$, respectively), regardless of the HL presence. **(B)** *En face* atherosclerosis analysis of aortic arch (left panel) and thoracic aorta (right panel) in Oil Red-O stained whole-mounted aorta of the four groups of mice. Atherosclerosis analysis in mice showed that, as previously described, HL inactivation reduced lesion size in *apoE-/- Irs2+/+HL+/+* mice fed 8 weeks atherogenic diet (*apoE-/-Irs2+/+HL-/- vs apoE-/-Irs2+/+HL+/+* mice $p=0.05$ and $p<0.007$). Consistent with previous results, atheroma lesion was significantly increased in the aortic arch of IR *apoE-/-Irs2+/-HL+/+* mice compared to *apoE-/-Irs2+/+HL+/+* mice ($p<0.01$). Inactivation of HL in IR mice diminished atherosclerosis development (*apoE-/-Irs2+/-HL-/- vs apoE-/- Irs2+/-HL+/+*, $p<0.0001$ and $p<0.003$) indicating a proatherogenic role of HL also in IR/MetS states. Data is presented as mean±sem. Statistical analysis was performed using One-way ANOVA analysis and only relevant statistics are shown.

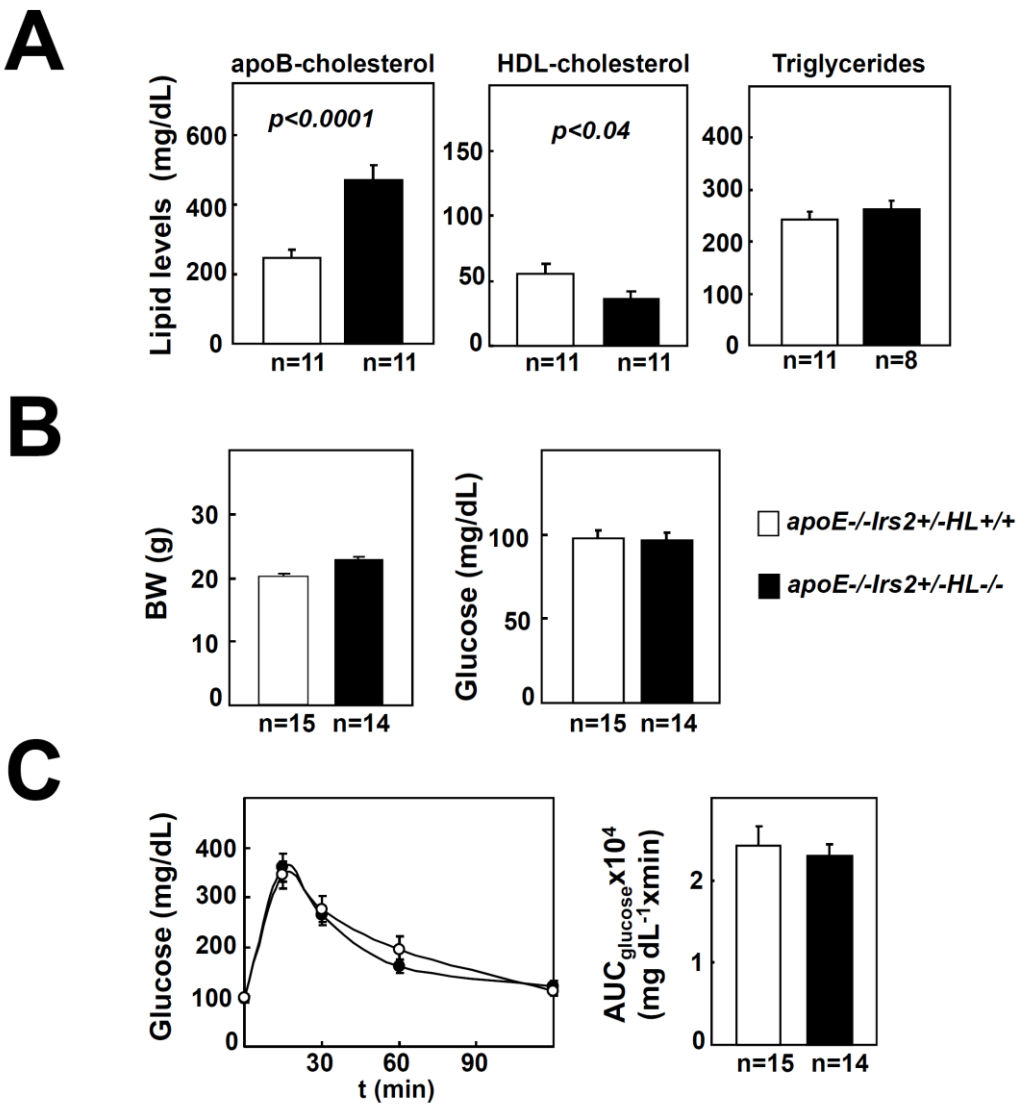

Suppl. Figure 2. Metabolic characterisation of *apoE-/-Irs2+/-HL+/+* and *apoE-/-Irs2+/-HL-/-* female mice fed atherogenic diet for 8 weeks. (A) ApoB–Cholesterol, HDL-Cholesterol and triglycerides plasma levels from both groups of mice. **(B)** Body weight (BW) and plasma glucose levels. **(C)** Plasmatic glucose levels during the glucose tolerance test (GTT) in *apoE-/-Irs2+/-HL+/+ vs apoE-/-Irs2+/-HL-/-* mice (left panel) and the area under the curve generated from the glucose measurements at different time points of the test ($AUC_{glucose,}$ right panel). Analysis of circulating lipid levels exhibited increased apoB-cholesterol and decreased HDL-Cholesterol in *apoE-/-Irs2+/-HL-/-* compared to *apoE-/-Irs2+/-HL+/+* mice. No changes were observed in triglycerides plasma levels, body weight, fasting glucose levels and glucose tolerance between both groups of mice. Data is presented as mean±sem. Statistical analysis was performed using Student's t-test analysis.

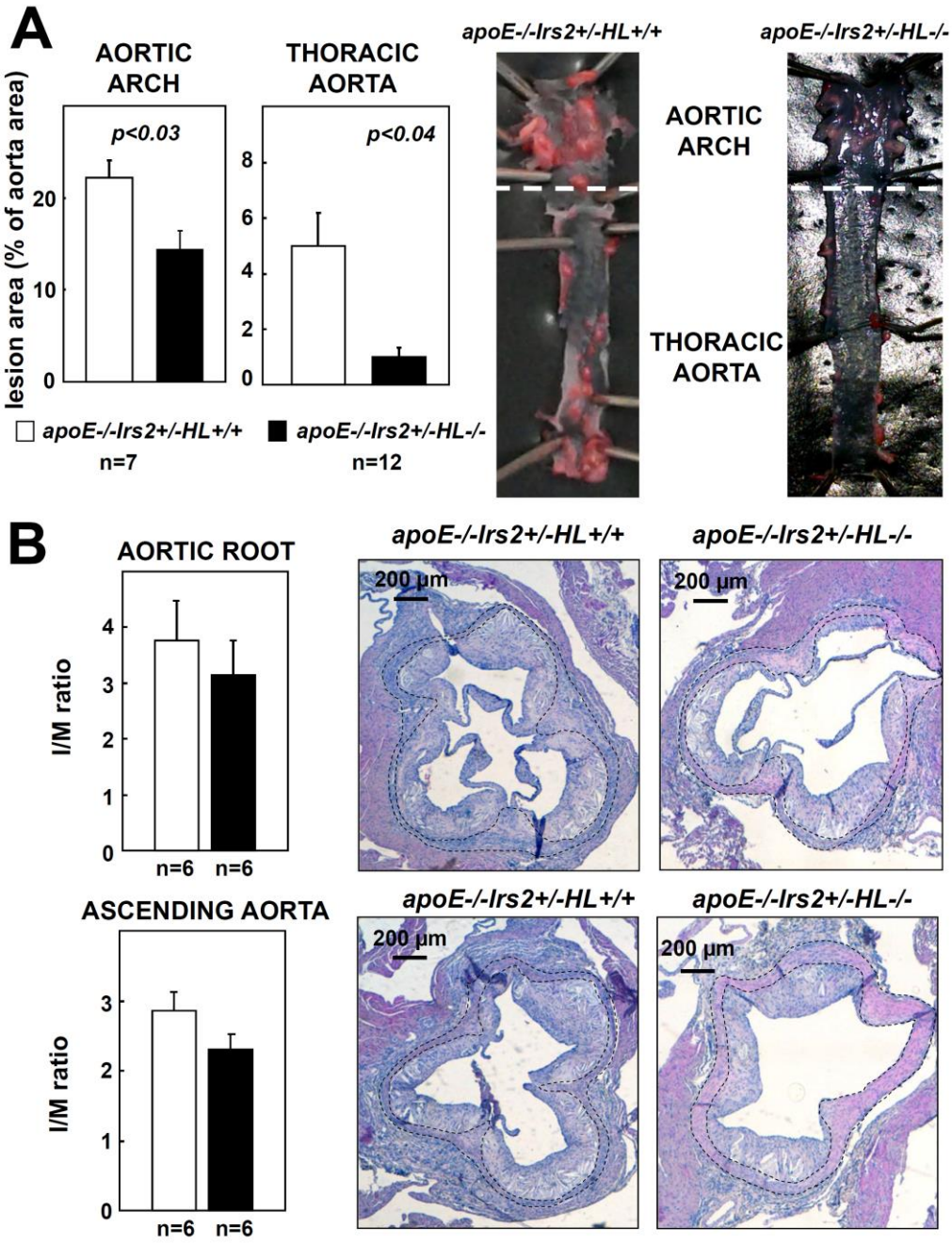

Suppl. Figure 3. Atherosclerotic lesion analysis of *apoE-/-Irs2+/-HL+/+* and *apoE-/-Irs2+/-HL-/-* female mice fed two months an atherogenic diet. (A) *En face* atherosclerosis analysis in Oil Red-O stained whole-mounted aorta from both groups of mice. **(B)** Atheroma lesion size measured as intima-media ratio in aortic root and ascending aorta (separated by 160 µm) from *apoE-/-Irs2+/-HL+/+* and *apoE-/-Irs2+/-HL-/-* mice. Representative photographs of aortas and images from hematoxylin/eosin stained cross-sections are shown. HL inactivation in *apoE-/-Irs2+/-* mice significantly decreased *en face* atheroma size. A not significant decreased was observed in atheroma lesion in aortic root and ascending aorta cross-sections. The discontinuous lines delineate the limits of the media. Statistical analysis was performed using Student's t-test analysis.

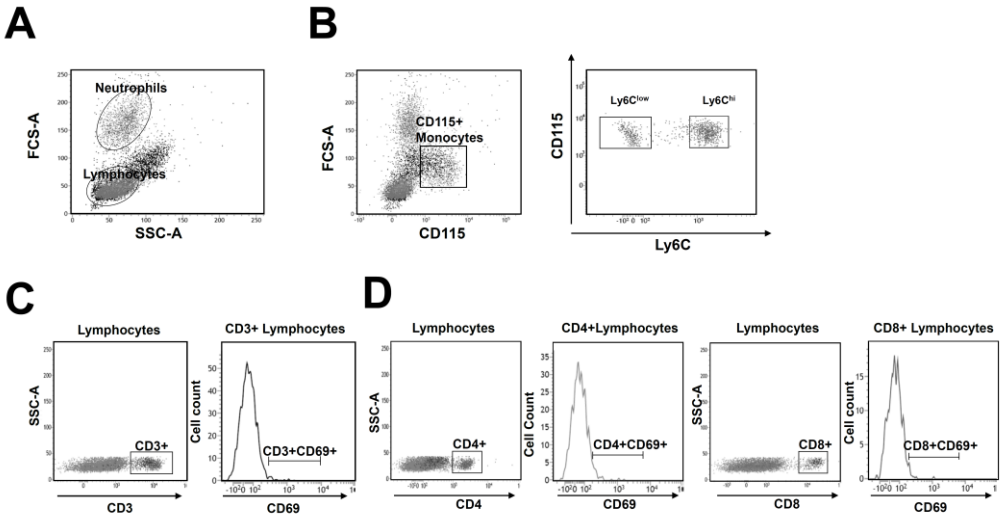

Suppl. Figure 4. Representative plots of the flow cytometry analysis of the circulating leukocyte used for *apoE-/-Irs2+/-HL+/+* and *apoE-/-Irs2+/-HL-/-* mice fed two months an atherogenic diet. **(A)** Representative plots of the gatings to determine the different populations of leukocytes in the blood. **(B)** Gating of monocytes as CD115+ cells and characterisation of CD115+Ly6C^{low} and CD115+Ly6C^{hi} monocyte subpopulations in both genotypes. **(C)** Representative plots of CD3+ and CD3+CD69+ T lymphocytes. **(D)** Representative plots of CD4+ and CD4+CD69+, CD8+ and CD8+CD69+, T lymphocyte subpopulations.

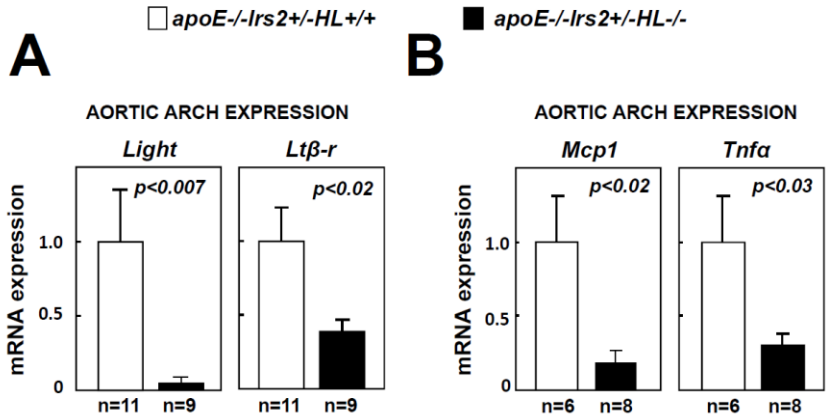

Suppl. Figure 5. Expression of inflammatory mediators in aortic arch from *apoE-/-Irs2+/-HL+/+* and *apoE-/-Irs2+/-HL-/-* mice. mRNA levels of **(A)** *Light*, *Ltβ-r*, **(B)** *Mcp1* and *Tnf-α* in aortic arch tissue from both groups of mice. mRNA levels were normalised to the endogenous *cyclophilin* expression and relativised to *apoE-/-Irs2+/-HL+/+* mouse mRNA levels. Statistical analysis was performed using the Student´s t-test.

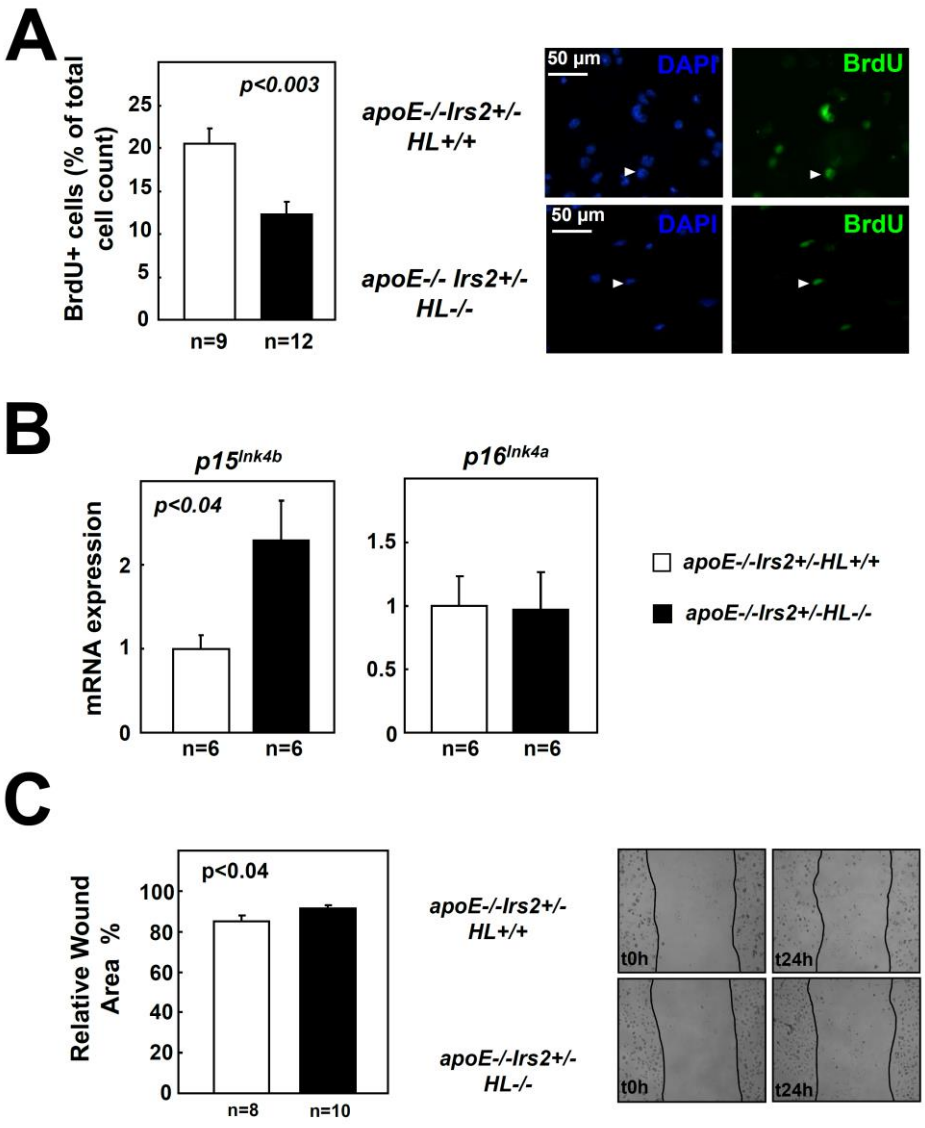

Suppl. Figure 6. ***In vitro*** **macrophage proliferation and migration analysis in** ***apoE-/-Irs2+/-HL+/+*** **and** ***apoE-/-Irs2+/-HL-/-*** **mice. (A)** Percentage of proliferating bone marrow-derived macrophages analysed by *in vitro* BrdU incorporation and detected by immunofluorescence. White arrows point to BrdU+ cells. **(B)** $p15^{Ink4b}$ and $p16^{Ink4a}$ mRNA expression from both groups of mice. **(C)** Quantification of wound-healing migration area from both groups of mice at time 24h relative to time 0h area. *ApoE-/-Irs2+/-HL-/-* mice displayed reduced proliferation and migration rate compared to *apoE-/-Irs2+/-HL+/+* mice coinciding with increased mRNA levels of the CDK4/6 inhibitor $p15^{Ink4b}$. Representative images at time 0h and 24h of the assay are shown. mRNA levels were normalised to the endogenous *cyclophilin* expression and relativised to *apoE-/-Irs2+/-HL+/+* mouse mRNA levels. Statistical analysis was performed using the Student´s t-test.

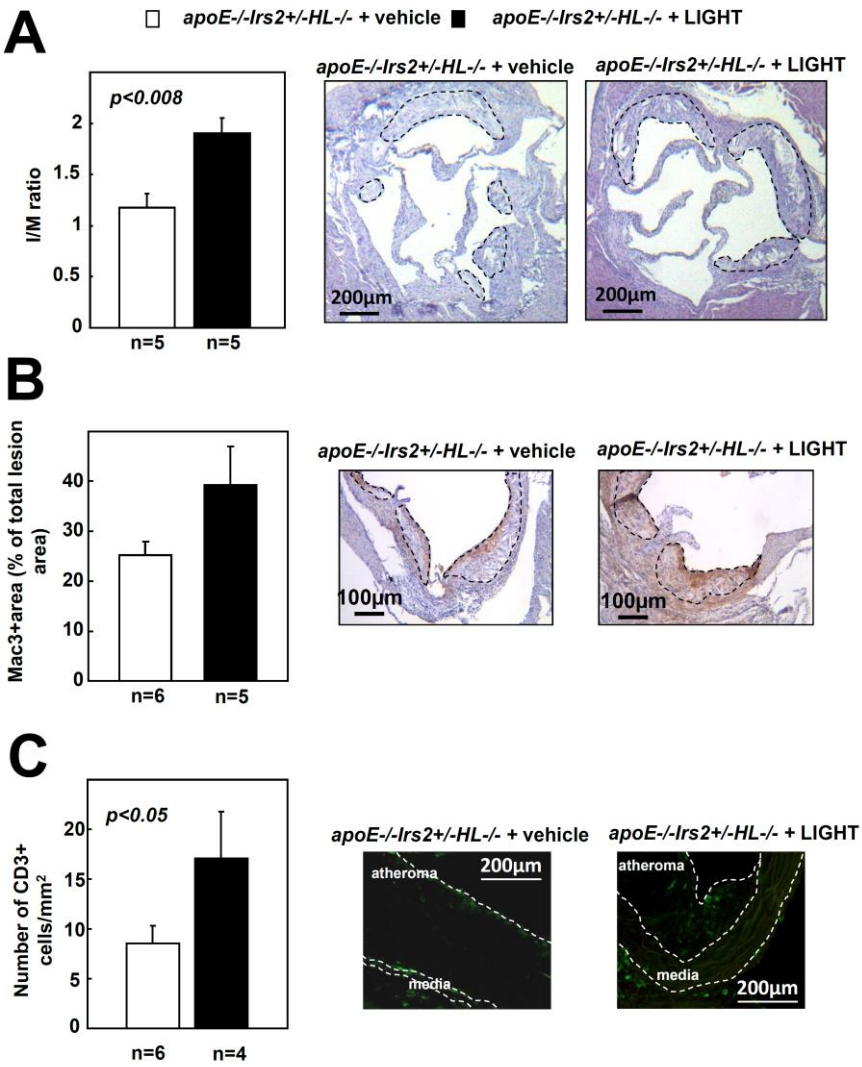

Suppl. Figure 7. Atheroma lesion analysis in aortic cross sections of atherogenic diet-fed *apoE-/-Irs2+/-HL-/-* mice treated with recombinant LIGHT or vehicle for one month. (A) Atheroma lesion size measured as intima-media ratio in aortic cross sections from vehicle and LIGHT-treated mice. Lesion size was increased in LIGHT-treated *apoE-/-Irs2+/-HL-/-* mice. **(B)** Neointimal content of macrophages (as percentage) and **(C)** T-lymphocytes (as number of cells/mm^2) using antibodies against specific markers (Mac-3 and CD3 respectively). T-lymphocyte content was increased in atheroma lesions of LIGHT-treated *apoE-/-Irs2+/-HL-/-* mice. Photomicrographs show representative images of the stainings and inmunofluorescences. The discontinuous lines delineate the limits of the media and atheromas. Statistical analysis was performed using Student's t-test analysis.

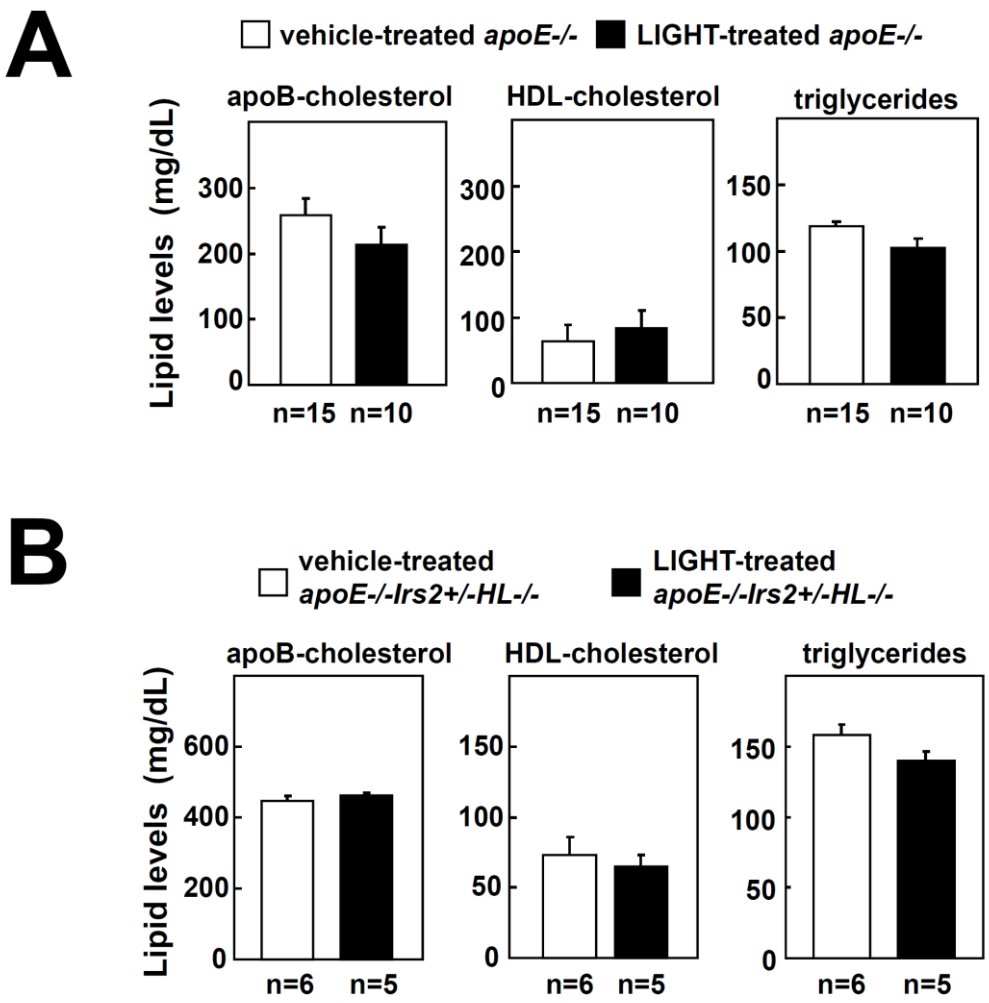

Suppl. Figure 8. Effect of LIGHT treatment on lipid levels in mice treated with LIGHT. (A) ApoB–cholesterol, HDL-cholesterol and triglycerides plasma levels in control-diet fed *apoE-/-* mice treated 5 days with vehicle or LIGHT. **(B)** ApoB–cholesterol, HDL-cholesterol and triglycerides plasma levels in 2 month atherogenic-diet fed *apoE-/-Irs2+/-HL-/-* mice treated with recombinant LIGHT or vehicle for one month. LIGHT treatment did not change plasma levels. Statistical analysis was performed using Student's t-test analysis.

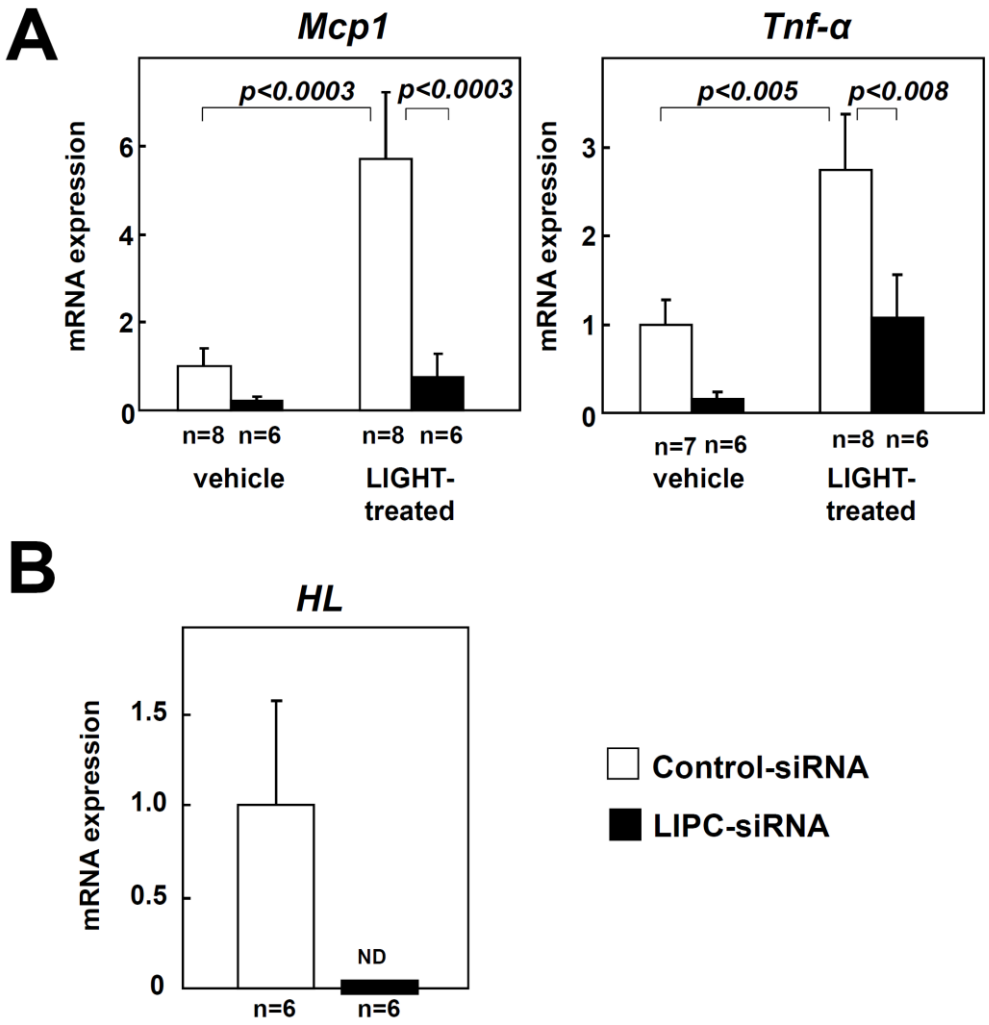

Suppl. Figure 9. Effect of LIGHT on Control-siRNA- and LIPC-siRNA-treated human macrophages. (A) mRNA expression analysis of *Mcp1* and *Tnfα* in vehicle and LIGHT-treated control-siRNA and LIPC-siRNA macrophages. mRNA levels were normalised with endogenous *gapdh* mRNA levels and relativised to vehicle-treated Control-siRNA mRNA levels. LIGHT enhanced *Mcp1* and *Tnfα* expression levels in Control-siRNA macrophages but these were unchanged upon silencing of *Hl* in LIPC-siRNA human macrophages**. (B)** *Hl* mRNA expression levels in Control-siRNA macrophages which were not detected (ND) in LIPC-siRNA-treated macrophages. mRNA levels were normalised with endogenous *gapdh* mRNA levels. Statistical analysis was performed by One-Way ANOVA **(A)** and Student's t-test **(B)**.

Suppl. References

1. González-Navarro H, Nong Z, Amar MJ, et al. The ligand-binding function of hepatic lipase modulates the development of atherosclerosis in transgenic mice. J Biol Chem 2004; 279: 45312-21.
2. Gonzalez-Navarro HV-C, M. Pastor, M-F. Vinue, A. White, M.F. , Burks DA, V. Plasma insulin levels predict the development of atherosclerosis when IRS2 deficiency is combined with severe
hypercholesterolemia in apolipoprotein E-null mice. Frontiers in Bioscience 2007; 12: 2291-8.
3. Martinez-Hervas S, Vinue A, Nunez L, et al. Insulin resistance aggravates atherosclerosis by reducing vascular smooth muscle cell survival and increasing CX3CL1/CX3CR1 axis. Cardiovasc Res 2014; 103: 324-36.
4. Gonzalez-Navarro H, Abu Nabah YN, Vinue A, et al. p19(ARF) deficiency reduces macrophage and vascular smooth muscle cell apoptosis and aggravates atherosclerosis. J Am Coll Cardiol 2010; 55: 2258-68.
5. Executive Summary of The Third Report of The National Cholesterol Education Program (NCEP) Expert Panel on Detection, Evaluation, And Treatment of High Blood Cholesterol In Adults (Adult Treatment Panel III). Jama 2001; 285: 2486-97.
6. Martinez-Hervas S, Argente C, Garcia-Jodar J, et al. Misclassification of subjects with insulin resistance and associated cardiovascular risk factors by homeostasis model assessment index. Utility of a postprandial method based on oral glucose tolerance test. Metabolism 2011; 60: 740-6.
7. Touboul PJ, Hennerici MG, Meairs S, et al. Mannheim intima-media thickness consensus. Cerebrovasc Dis 2004; 18: 346-9.
8. Kuo CL, Murphy AJ, Sayers S, et al. Cdkn2a is an atherosclerosis modifier locus that regulates monocyte/macrophage proliferation. Arterioscler Thromb Vasc Biol 2011; 31: 2483-92.
9. Rogacev KS, Cremers B, Zawada AM, et al. CD14++CD16+ monocytes independently predict cardiovascular events: a cohort study of 951 patients referred for elective coronary angiography. J Am Coll Cardiol 2012; 60: 1512-20.
10. Eligini S, Crisci M, Bono E, et al. Human monocyte-derived macrophages spontaneously differentiated in vitro show distinct phenotypes. J Cell Physiol 2013; 228: 1464-72.
11. Gonzalez-Navarro H, Vinue A, Sanz MJ, et al. Increased dosage of Ink4/Arf protects against glucose intolerance and insulin resistance associated with aging. Aging Cell 2013; 12: 102-11.